Nanoscale Research Letters
a SpringerOpen Journal

NANO EXPRESS Open Access

The MoS_2 Nanotubes with Defect-Controlled Electric Properties

Maja Remskar[1*], Ales Mrzel[1], Marko Virsek[1], Matjaz Godec[2], Matthias Krause[3], Andreas Kolitsch[3], Amol Singh[4], Alan Seabaugh[4]

Abstract

We describe a two-step synthesis of pure multiwall MoS_2 nanotubes with a high degree of homogeneity in size. The $Mo_6S_4I_6$ nanowires grown directly from elements under temperature gradient conditions in hedgehog-like assemblies were used as precursor material. Transformation in argon-H_2S/H_2 mixture leads to the MoS_2 nanotubes still grouped in hedgehog-like morphology. The described method enables a large-scale production of MoS_2 nanotubes and their size control. X-ray diffraction, optical absorption and Raman spectroscopy, scanning electron microscopy with wave dispersive analysis, and transmission electron microscopy were used to characterize the starting $Mo_6S_4I_6$ nanowires and the MoS_2 nanotubes. The unit cell parameters of the $Mo_6S_4I_6$ phase are proposed. Blue shift in optical absorbance and metallic behavior of MoS_2 nanotubes in two-probe measurement are explained by a high defect concentration.

Introduction

One-dimensional nanostructures such as nanorods, nanobelts, nanowires and nanotubes have attracted intensive attention due to their unique applications in mesoscopic physics and nanoscale devices. In analogy to graphite, nanoparticles of many two-dimensional inorganic compounds are unstable against folding and can form closed cage structures which are referred to as inorganic fullerene-like particles and inorganic nanotubes[1]. Recent discovery of MoS_2 nanopods called "mama"-tubes [2] with MoS_2 fullerene-like particles in-situ grown in a confined geometry of MoS_2 nanotubes and coaxial MoS_2 nanotube hybrids [3] have opened a new way of synthesis of MoS_2 nanotubes from $Mo_xS_yI_z$ ternary compounds, which allows for the production of mass quantities of nanomaterials. Weak van der Waals interactions among MoS_2 molecular layers enable low-strength shearing and several possible stackings [2,4].

Molybdenum disulfide nanostructures are receiving considerable attention because of their potential applications as heterogeneous catalysts for desulfurization processes [5], hydrogen evolution [6,7], and as materials for thermoelectric applications [8]. MoS_2 microplatelets have been used as a solid lubricant or as an additive in oil or grease for more than 60 years. Cage-like nanostructures, e.g. cylindrical MoS_2 nanotubes, represent a new generation of lubricants with extremely low friction resulting from the size, small enough to turn microvoids and nanovoids of the objects in mechanical contact into lubricant reservoirs, and by the curved geometry of the nanoparticles, which put them into constantly parallel orientation with the counterpart surfaces. The orientation relationship has been proposed to explain the ultra-low friction measured on thin films composed of MoS_2 fullerene-like particles even at high humidity [9]. Lubrication is strongly related to electronic properties, more precisely to the filling of Mo d_{z^2} molecular orbitals [10]. Control of nanotube dimensions and the density of defects that influence transport properties are of great importance in the construction of nanoscale electronic devices and multifunctional materials.

The significantly lower molecular mass of MoS_2 in comparison with WS_2 is an advantage for many applications, although MoS_2 nanotubes are found to be more difficult to fabricate. Several different growth techniques are used for the synthesis of multiwall MoS_2 inorganic nanotubes, like sulfurization of molybdenium oxides [11,12] and chlorides [13] in a stream of H_2S gas, thermal decomposition of $(NH_4)_2MoS_4$ [14] and by the

* Correspondence: maja.remskar@ijs.si
[1]Jozef Stefan Institute, Jamova 39, 1000, Ljubljana, Slovenia.
Full list of author information is available at the end of the article

template method [15], hydrothermal synthesis [16] and chemical transport reaction using iodine as a transport agent [17]. Currently, most of the described techniques are not suitable for large-scale production of pure multiwall MoS_2 nanotubes, which would possess a relatively uniform size.

In the present paper, we report on a synthesis that can be scaled up for bulk production of pure multiwall MoS_2 nanotubes of lengths up to several tens micrometers and diameters up to 100 nm using groups of $Mo_6S_4I_6$ nanowires as precursor crystals. The structural data are combined with optical absorbance and Raman scattering. In addition, two-probe current–voltage measurements were performed on a single nanotube.

Experimental

Sample Preparation

The $Mo_6S_4I_6$ nanowires were fabricated in evacuated (10^{-4} Pa) quartz ampoules directly from molybdenum and sulfur powder (Aldrich, 99.98 %), and iodine flakes (99.999%, Aldrich) in a molar ratio of 6: 3: 9. The iodine was used as the transport agent in the chemical transport reaction, which took place in a two-zone horizontal furnace for 48 h under a temperature gradient of 5.5 K/cm. A fraction (5–10 wt.%) of the total synthesized material was transported to the low-temperature zone (1010 K) of the ampoule and grew in the form of a hairy foil composed of $Mo_6S_xI_y$ nanowires with some traces of MoI_2 at the interface with the quartz, while the material remaining at the hot zone (1123 K) appeared as a dark-brown powder. The stoichiometry of this remaining powder in the form of $Mo_6S_4I_6$ nanowires was determined by wave dispersive analysis using a scanning electron microscope, Jeol JSM 6500F. These nanowires were used as the precursor material for transformation into MoS_2 nanotubes by annealing at 1073 K in the reactive gas composed of 98 vol% of Ar, 1 vol% of H_2S, and 1 vol% of H_2 for 1 h. In a typical experiment, around 600 mg of the starting material was sulfurized and transformed into MoS_2 nanotubes. The total mass of the starting material during the transformation was decreased for 40% due to the complete removal of iodine and its substitution by the lighter sulfur. X-ray powder diffraction and X-ray energy dispersive analysis of the end product reveal the iodine-free MoS_2 compound.

Characterization

The $Mo_6S_4I_6$ precursor crystals and MoS_2 nanotubes have been studied by high-resolution 200 keV Jeol 2010 F field-emission transmission electron microscopes (HRTEM) and scanning electron microscope FE-SEM, Supra 35 VP, Carl Zeiss. X-ray diffraction (XRD), optical absorption, Raman spectroscopy, and wave dispersive analysis (WDS) were used to characterize the obtained materials. X-ray diffraction (XRD) was performed at room temperature with a D4 Endeavor diffractometer (Bruker AXS) using quartz monochromator Cu Kα1 radiation source (λ = 0.1541 nm) and Sol-X energy dispersive detector. Angular range 2 θ was chosen from 6° to 73° with a step size of 0.04° and a collection time of 4 s. The samples were rotated during measurements at 6 rpm. Raman spectra were recorded in a micro-Raman 180° backscattering configuration on a Labram HR spectrometer with a spectral resolution of 1.5 cm^{-1} determined by the width of 3 CCD-pixels. For excitation, a frequency-doubled Nd:YAG 532 nm laser operated with 100 μW power on the sample was used. Under these conditions, heating or degradation effects were excluded. Transport properties were measured using an Agilent 4155 semiconductor parameter analyzer using on-wafer probing of two-terminal test structures.

Results and Discussion

The $Mo_6S_4I_6$ Nanowires

$Mo_6S_4I_6$ nanowires grew as hedgehog-like self-assemblies (Figure 1a) composed of nanowires of very homogeneous size, up to 100 nm in diameter and up to 20 μm in length. Considering that little information is available about this phase with no unit cell determined [18], we describe the direction of growth and assignment of the diffraction pattern in accordance with the similar $Mo_6S_2I_8$ phase [19]. We find close similarities of electron and X-ray diffraction patterns of both phases, which generalize the report [20] on the stability of the $Mo_6S_{9-x}I_x$ nanowires ($4.5 < x < 6$) with different S and I stoichiometries, to the $Mo_6S_4I_6$ phase. Nanowires of different stoichiometries grow in skeletal structures composed of one-dimensional polymer chains of Mo_6–chalcogen–halogen clusters, which differ only in the site occupation by sulfur and iodine. This makes difficulties in the determination of a particular phase, especially based on X-ray results. In our studies, we used electron diffraction obtained on a single nanowire for the elucidation of the symmetry rules, X-ray diffraction for the determination of interlayer distance with sufficient accuracy, and wave dispersive analysis for the determination of the stoichiometry on a single nanowire. Due to a mixed range of selective area diffraction, one cannot exclude the presence of other $Mo_6S_{9-x}I_x$ and $Mo_6S_{10-x}I_x$ nanowires in the starting materials, like $Mo_6S_3I_6$ or $Mo_6S_2I_8$ [20]. Nevertheless, most of the starting materials can be attributed to one phase, i.e. $Mo_6S_4I_6$, while the others incorporate impurities that cause broadening of the X-ray peaks.

The $Mo_6S_4I_6$ nanowires possess a high aspect ratio and grow in a longitudinal direction along the [001]. The needles are rigid and well crystallized (Figure 1b). One-dimensional chains are mutually ordered and in contrast with reported $Mo_6S_3I_6$ nanowires do not

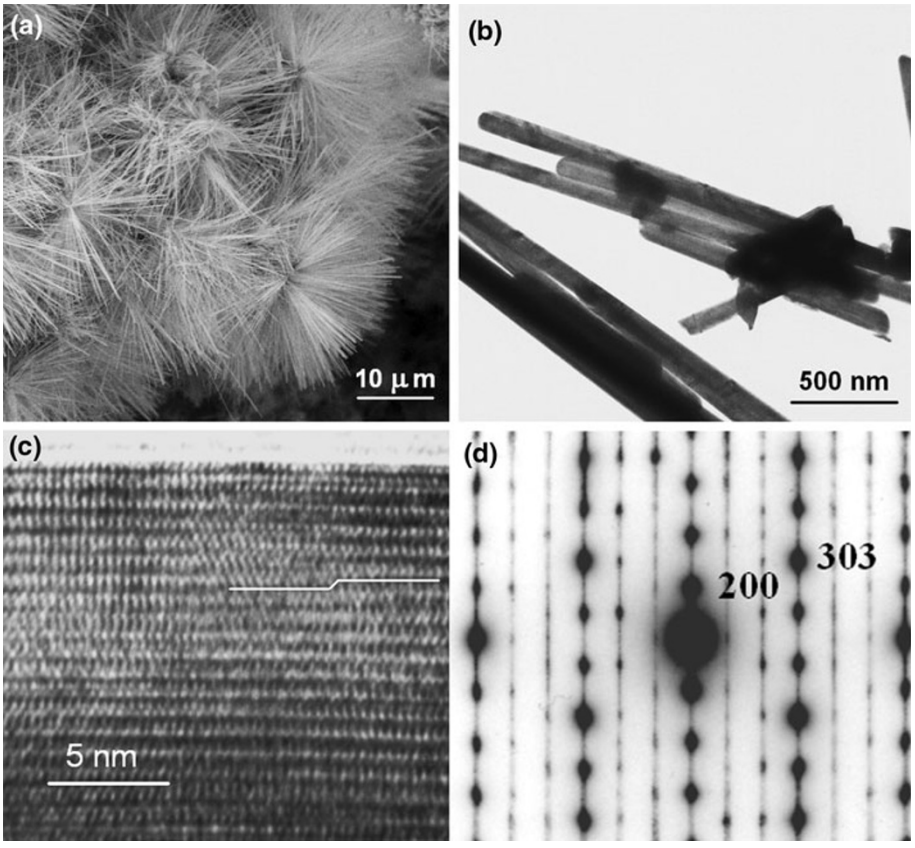

Figure 1 The $Mo_6S_4I_6$ nanowires: a A SEM image of hedgehog-like self-assemblies of identical nanowires grown up to 10 μm in length; b A TEM image revealing rigid nanocrystals with dome terminations; c A HRTEM image with *rows* of Mo_6 clusters surrounded by sulfur and iodine atoms. A stacking fault in otherwise regular order is marked with a stepped line and associated with a disordered structure; **d** TED pattern of a single $Mo_6S_4I_6$ nanowire in the [010] zone assigned in accordance with the proposed space group $P6_3/m$ and lattice parameters of a hexagonal structure with: a = 1.88(5) nm and c = 1.18 nm.

exhibit a tendency for easy splitting. A stacking fault marked in Figure 1c with the component of the Burger's vector perpendicular to the nanowires axis can contribute to the resistance of the needles against longitudinal cleavage and decreases a strong anisotropy of these quasi one-dimensional cluster compounds.

The electron diffraction pattern of a single $Mo_6S_4I_6$ nanowire (Figure 1d) is assigned in accordance with the proposed space group $P6_3/m$ and estimated lattice parameters of a hexagonal structure with: a = 1.88(5) nm and c = 1.18 nm. The nanowires grow with the [001] axis along their longitudinal direction.

Besides $Mo_6S_4I_6$ nanowires, X-ray investigation of the starting material (Figure 2a-A) reveals the presence of the $Mo_6S_2I_8$ and traces of MoS_2. The (002) MoS_2 peak is shown by an asterisk in spectrum (a), while other MoS_2 peaks cannot be resolved. Due to nearly identical skeletal structures, most of the diffraction peaks of $Mo_6S_4I_6$ and $Mo_6S_2I_8$ nearly match, leading to a broadening of the peaks in addition to the size effect broadening. As an example, the peak at ~.817 nm is composed of two peaks situated at 0.816(1) nm and at 0.825(8) nm. The last one can be associated with the $Mo_6S_2I_8$ (110) planes, while the first one was used for the approximation of the unknown unit cell of $Mo_6S_4I_6$ nanowires. The symmetry of the TED pattern (Figure 1d) was utilized for assignation of the peak to the (200) planes of the $Mo_6S_4I_6$. The peak positioned at 0.197 nm was associated with the (006) planes. Complete determination of the $Mo_6S_4I_6$ structure needs further studies.

Transformation of the $Mo_6S_4I_6$ Nanowires into MoS_2 Nanotubes

The X-ray powder diffraction of the product after the transformation (Figure 2a-B) reveals the iodine-free MoS_2 compound. The spectrum is assigned according to the MoS_2 (JCPDS-No. 77-1716). The Raman spectra of $Mo_6S_4I_6$ nanowires are shown in Figure 2b-B and is almost identical with that of the pure $Mo_6S_2I_8$

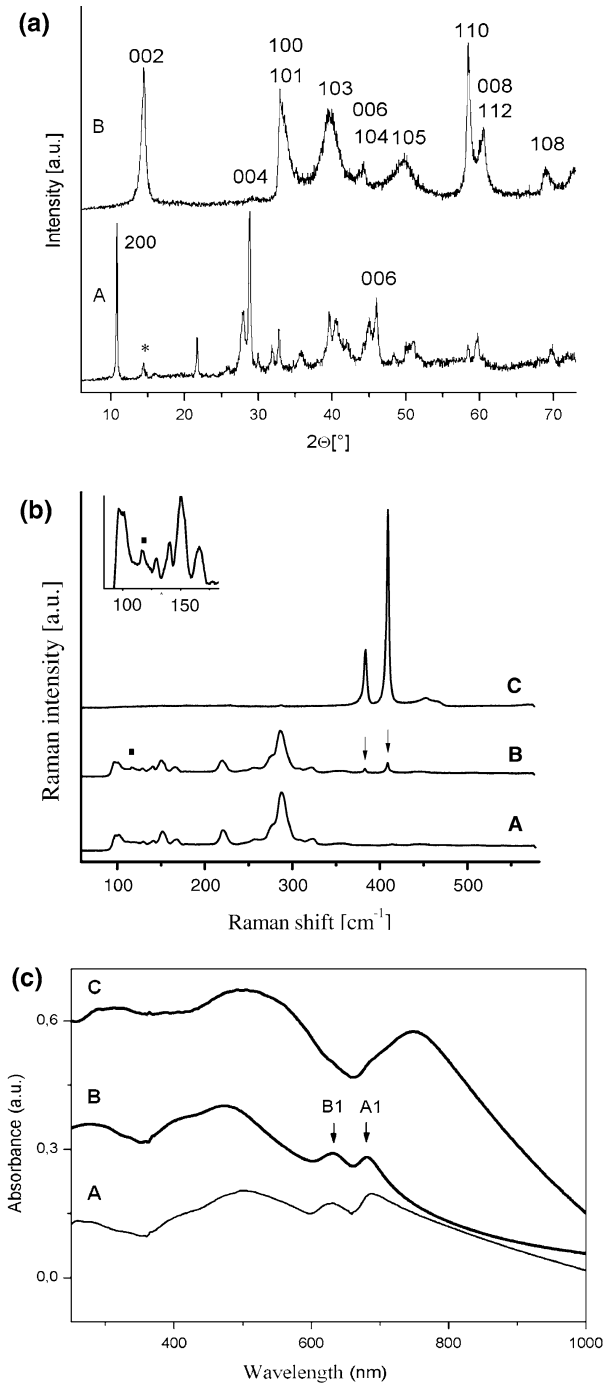

Figure 2 a X-ray powder diffraction pattern (*A*) The starting material composed of $Mo_6S_4I_6$ nanowires with traces of MoS_2 (*asterisk*) and $Mo_6S_2I_8$. The two *indexed peaks* are used for approximation of the unit cell of $Mo_6S_4I_6$; (*B*) The final material is composed of pure multiwall MoS_2 nanotubes. **b** Raman spectra: (*A*) $Mo_6S_2I_8$ nanowires, (*B*) $Mo_6S_4I_6$ nanowires; *arrows* point traces of MoS_2; square dot (see also the *inset*) shows a position of the characteristic peak at 117 cm^{-1}, (*C*) MoS_2 nanotubes gained by sulfurization of $Mo_6S_4I_6$ nanowires. **c** Optical absorption spectra: (*A*) $Mo_6S_4I_6$ precursor nanowires; (*B*) MoS_2 nanotubes; (*C*) MoS_2 polycrystalline material (*powder*). All materials were dispersed in ethanol.

(Figure 2b-A). The only exception is the relative intensity of the peak at 117 cm^{-1}, which is higher in the $Mo_6S_4I_6$ compared to the $Mo_6S_2I_8$. Some traces of MoS_2 could also be observed in some spectra, marked by arrows. The spectroscopic similarity is a further support for the nearly identical crystal and local structure of $Mo_6S_4I_6$ and $Mo_6S_2I_8$. The Raman spectrum of the final product-MoS_2 nanotubes (Figure 2b-C) contains the usual signature of MoS_2, A_{1g} mode at 409 cm^{-1} and E_{2g} mode at 384 cm^{-1} [21]. No traces of precursor $Mo_6S_4I_6$ nanowires are observed. A small peak at the 287 cm^{-1} is attributed to the MoS_2, E_{1g} mode that is forbidden in the backscattering experiments on the basal (001) plane. The reason for E_{1g} occurrence is the cylindrical geometry with a great part of the basal planes oriented in parallel with the axis of illumination. The line widths of the MoS_2 nanotubes are larger than that of MoS_2 single crystals. The FWHM of the A_{1g} line increases from 2.0 to 3.3 cm^{-1} and that of the E_{2g} from 1.6 to 3.8 cm^{-1}. The line broadening is attributed to a smaller crystallite size and to a larger amount of defects in multiwall MoS_2 nanotubes compared to MoS_2 single crystals [22,23].

The electronic band structure calculations show that the bulk MoS_2 is an indirect gap semiconductor with two exciton absorption bands at the absorption edge [24]. The absorption associated with the direct band gap is located in the visible spectrum around 700 nm and results from a direct transition at the K point. Two peaks assigned as A1 (690 nm) and B1 (620 nm) are attributed to two excitons of the Rydberg series. The band at around 500 nm is associated with the direct transitions from the valence band to the conduction band [25].

UV-Vis absorption spectroscopy was performed at room temperature. The MoS_2 powder, $Mo_6S_4I_6$ nanowires, and MoS_2 nanotubes were ultra-sonicated in ethanol. MoS_2 powder (Aldrich) was used as a reference material. The UV-Vis absorption spectrum (Figure 2c) of the $Mo_6S_4I_6$ nanowires (A) reveals two broad peaks at 748 nm (1.66 eV) and 487 nm (2.55 eV). The absorption spectrum of the MoS_2 nanotubes (B) reveals the A1 peak occurring at 681 nm and B1 at 631 nm with energy separation of 0.14 eV. The third peak dominates the spectrum, and it is blue-shifted with respect to MoS_2. It is composed of a peak at 472 nm (2.63 eV) and its shoulder at 416 nm (2.99 eV). Comparison with the spectrum obtained by dispersed MoS_2 powder in the form of platelets (C) reveals two main differences in the MoS_2 nanotube sample: (i) a decrease in energy separation between A1 and B1 associated with the spin-orbit splitting of the top of the valence gap at the K point [20] and (ii) a blue shift, relative intensity and the shape of the

absorption peak centered at the 472 nm, revealing changes in the direct transitions from the valence band to the conduction band. Besides these differences, the spectrum of MoS_2 nanotubes matches well with the spectrum belonging to the dispersed MoS_2 polycrystalline sample.

Morphology of MoS_2 Nanotubes

The MoS_2 multiwall nanotubes gained by the sulfurization after complete iodine removal keep the shape of the precursor $Mo_6S_4I_6$ nanowires (Figure 3a). The nanotubes are still organized in hedgehog-like groups (Figure 3b). The tube walls with a typical thickness below 10 nm are strongly defected (Figure 3c). The lattice defects condensate forming faceting of the dome closure or disorder areas near stacking faults of MoS_2 layers. Some inner cylinders can be terminated by curved players of outer cylinders (Figure 3d) revealing a dominant tendency of self-termination of surface molecular layers, while the inner ones did not gain sufficient energy for a closure.

Transport Measurement on a Single MoS_2 Nanotube

Two-terminal device was fabricated from MoS_2 nanotubes to measure transport properties (Figure 4a). The tubes were placed on a thermally-oxidized, heavily-doped p-Si substrate with a 90-nm-thick SiO_2 overlayer. Titanium/gold contacts 20/220 nm in respective thickness were formed by electron beam evaporation using a photolithographic lift-off process with separations between the electrodes of 5 μm. Two-terminal measurements on a MoS_2 nanotube, 105 nm in diameter, show a metallic (approximately ohmic) conduction. No photoconductivity was observed between measurements taken in the dark and under strong microscope illumination using a halogen lamp (Figure 4b). In addition, the wire conductivity could not be modulated independently on light illumination when backgated through the p + Si substrate in the range from -50 to +50 V with a tube bias ranging from 0 to 5 V, consistent with the metallic character of the nanotube. The nanotube conductivity is estimated to about 2 mS/cm by assuming that the wall thickness is 10 nm, which is the most frequently

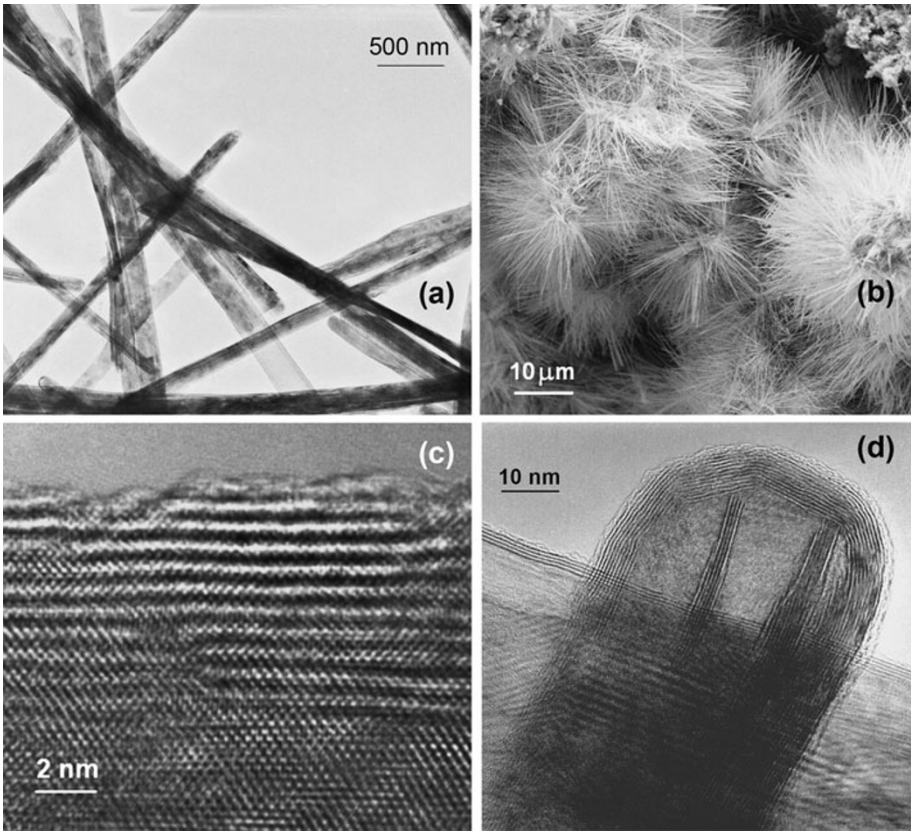

Figure 3 The MoS_2 nanotubes: a A typical TEM image of a bunch of nanotubes grown from sacrificed $Mo_6S_4I_6$ nanowires keeping their outer geometry; and b self-organization in hedgehock-like groups revealed by SEM; c HRTEM image of a nanotube's wall with resolved MoS_2 molecular layers, stacking faults and atomically rough surface; d TEM image of a single nanotube cap of a nanotube with inner cylinders terminated by curved layers of outer cylinders.

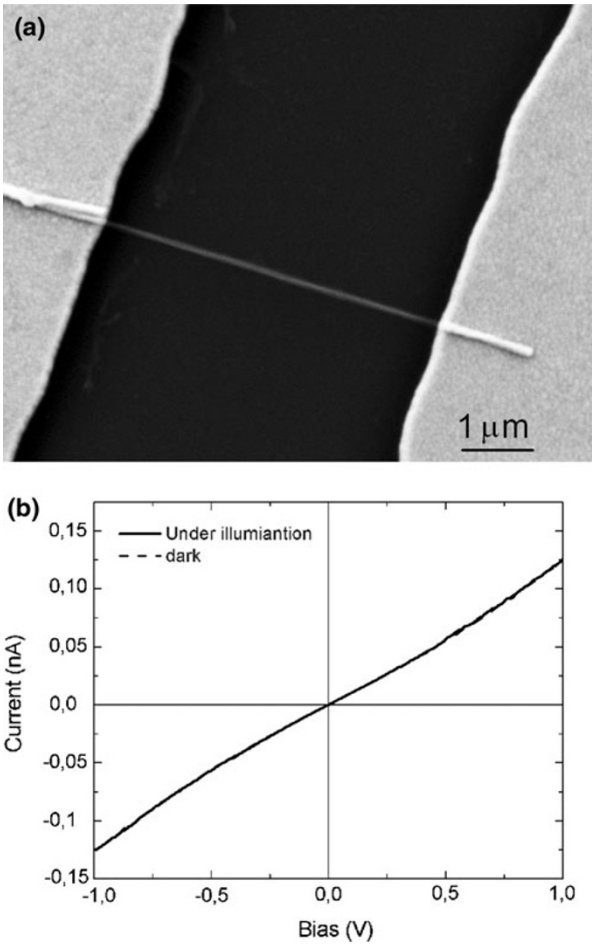

Figure 4 a Scanning electron micrograph of a MoS_2 nanotube between Ti/Au metal electrodes; b Current–voltage characteristics in the dark and under illumination for the MoS_2 nanotube at room temperature with and without visible light illumination.

observed value in these nanotubes. The metallic conductivity could indicate a high density of defects, which form energy states near the Fermi level and influence also the optical absorbance spectra.

Conclusion

In conclusion, we have reported an easy and straightforward way of fabricating pure multiwall MoS_2 nanotubes using $Mo_6S_4I_6$ nanowires as the precursor crystals. We synthesized the nanowires from elements in a furnace gradient and proposed the unit cell of the $Mo_6S_4I_6$ compound, which was first reported in 1985. The nanotubes produced by the sulfurization process keep the outer geometry and self-assembly of the precursor nanowires. They are of relatively homogeneous size in diameter and length. The lattice structure is strongly defected causing Raman line broadening, a blue shift in visible light absorption and metallic conductivity at room temperature of this otherwise semiconducting compound. The synthesis, which can be easily scaled up, and peculiar energy level distribution in these MoS_2 nanotubes could find application in nanoelectronics and tribology.

Author details
[1]Jozef Stefan Institute, Jamova 39, 1000, Ljubljana, Slovenia. [2]Institute of Metals and Technology, Lepi Pot 11, 1000, Ljubljana, Slovenia. [3]Forschungszentrum Dresden-Rossendorf, Institut für Ionenstrahlphysik und Materialforschung, D-01314, Dresden, Germany. [4]Department of Electrical Engineering, University of Notre Dame, Notre Dame, IN 46556, USA.

Received: 21 July 2010 Accepted: 16 August 2010
Published: 3 September 2010

References

1. Tenne R: *Nat Nanotechnol* 2006, **1**:103.
2. Remskar M, Mrzel A, Virsek M, Jesih A: *Adv Mater* 2007, **19**:4276.
3. Remskar M, Virsek M, Mrzel A: *Apply Phys Lett* 2009, **95**:133122.
4. Remskar M, Skraba Z, Ballif C, Sanjines R, Levy F: *Surf Sci* 1999, **433–435**:637.
5. Lauritsen J, Kibsgaard J, Helveg S, Topsoe H, Clausen BS, Lægsgaard E, Besenbacher F: *Nat Nanotechnol* 2007, **2**:53.
6. Hinnemann B, Moses PG, Bonde J, Jorgensen KP, Nielsen JH, Horch S, Chorkendorff I, Norskov JK: *J Am Chem Soc* 2005, **127**:5308.
7. Jaramillo TF, Jørgensen KP, Bonde J, Nielsen JH, Horch S, Chorkendorff I: *Science* 2007, **317**:100.
8. Chiritescu C, Cahill DG, Nguyen N, Johnson D, Bodapati A, Keblinski P, Zschack P: *Science* 2007, **315**:351.
9. Chhowalla M, Amaratunga GAJ: *Nature* 2000, **407**:164.
10. El Beqqali O, Zorkani I, Rogemond F, Chermette H, Ben Chaabane R, Gamoudi M: *Guiilaud Synth Metals* 1997, **90**:165.
11. Feldman Y, Wasserman E, Srolovitz DJ, Tenne R: *Science* 1995, **267**:222.
12. Therese HA, Zink N, Kolb U, Tremel W: *Solid State Sci* 2006, **8**:1133.
13. Deepak FL, Margolin A, Wiesel I, Bar-Sadan M, Popovitz-Biro R, Tenne R: *Nano* 2006, **1**:167.
14. Chen J, Li SL, Xu Q, Tanaka K: *Chem Commun* 2002, **16**:1722.
15. Rivera-Munoz EM: *J Appl Phys* 2007, **102**:094302.
16. Lavayen V, Mirabal N, O'Dwyer C, Ana MAS, Benavente E, Torres CMS, Gonzalez G: *Appl Surf Sci* 2007, **253**:5185.
17. Remskar M, Skraba Z, Cleton F, Sanjines R, Levy F: *Appl Phys Lett* 1996, **69**:351.
18. Drobot DV, Starkov VV, Pisarev EA: *Russ J Inorg Chem* 1985, **30**:1668.
19. Perrin C, Sergent M: *J Chem Res (S)* 1983, 38.
20. Meden A, Kodre A, Padeznik Gomilsek J, Arcon I, Vilfan I, Vrbanic D, Mrzel A, Mihailovic D: *Nanotechnology* 2005, **16**:1578.
21. Sandoval SJ, Yang D, Frindt RF, Irwin JC: *Phys Rev B* 1991, **44**:8.
22. Virsek M, Krause M, Kolitsch A, Mrzel A, Iskra I, Skapin SD, Remskar M: *J Phys Chem C* 2010, **114**:6458.
23. Frey GL, Tenne R, Matthews MJ, Dresselhaus MS, Dresselhaus G: *Phys Rev B* 1999, **60(4)**:2883.
24. Coehoorn R, Hass C, Dijkstra J, Flipse CJF: *Phys Rev B* 1987, **35**:6195.
25. Wilcoxon JP, Newcomer PP, Samara GA: *J Appl Phys* 1997, **81**:7934.

doi:10.1007/s11671-010-9765-0
Cite this article as: Remskar *et al.*: The MoS_2 Nanotubes with Defect-Controlled Electric Properties. *Nanoscale Res Lett* 2011 **6**:26.